Chapter 3
Analysis of Horizontal Thin-Wire Conductor Buried in Lossy Ground: New Model for Sommerfeld Type Integral

Milica Rančić, Radoslav Jankoski, Sergei Silvestrov and Slavoljub Aleksić

Abstract A new simple approximation that can be used for modeling of one type of Sommerfeld integrals typically occurring in the expressions that describe sources buried in the lossy ground, is proposed in the paper. The ground is treated as a linear, isotropic and homogenous medium of known electrical parameters. Proposed approximation has a form of a weighted exponential function with an additional complex constant term. The derivation procedure of this approximation is explained in detail, and the validation is done applying it in the analysis of a bare conductor fed in the center and immersed in the lossy ground at arbitrary depth. Wide range of ground and geometry parameters of interest has been taken into consideration.

Keywords Current distribution · Horizontal conductor · Integral equation · Lossy ground · Point-matching method · Sommerfeld integral

3.1 Introduction

Significant effort has been put into evaluation of the influence of real ground parameters on the near- and far-field characteristics of wire conductors (or systems consisting of them) located in the air above lossy ground, or buried inside of it [1–8, 10–22,

M. Rančić (✉) · S. Silvestrov
Division of Applied Mathematics, The School of Education, Culture and Communication, Mälardalen University, Box 883, 721 23 Västerås, Sweden
e-mail: milica.rancic@mdh.se

S. Silvestrov
e-mail: sergei.silvestrov@mdh.se

R. Jankoski
FEIT, Ss. Cyril and Methodius University, Skopje, Macedonia
e-mail: radoslavjankoski@gmail.com

S. Aleksić
Faculty of Electronic Engineering, University of Niš, Niš, Serbia
e-mail: slavoljub.aleksic@elfak.ni.ac.rs

S. Silvestrov and M. Rančić (eds.), *Engineering Mathematics I*,
Springer Proceedings in Mathematics & Statistics 178,
DOI 10.1007/978-3-319-42082-0_3

24–37]. The methods applied in this research field range from simplified analytical to rigorous full-wave ones.

The one often used in cases of conductors buried in the ground is the transmission line model (TLM) [3, 16, 17, 20], which offers advantages of analytical approaches: simplicity and short calculation time. However, the TLM introduces calculation errors depending on the electrical properties of the ground, burial depth, and frequency range in question. More specifically, it is reliable for deep-buried long horizontal conductors at frequencies below MHz range, [16, 17, 20].

On the other hand, using the full-wave approach [1, 4–6, 12–15, 18, 19, 21], any kind of arbitrarily positioned wire system could be analyzed, at any frequency of interest with no restrictions to the electrical parameters of the ground. This approach is based on formulation of the electric field integral equation (EFIE) and its solution using an appropriate numerical method (e.g. method of moments, boundary element method). The influence of the ground parameters is taken into account through Sommerfeld integrals, which are a part of the kernel of the formulated integral equation (e.g. Pocklington, Hallén, etc.). Although the calculation accuracy that comes with this approach is high, greater computational costs also need to be paid, which depends on the numerical method used for EFIE solving, and the way Sommerfeld integrals are dealt with.

Basically, two approaches can be taken for the latter issue. The first, more time-consuming one, but also the one yielding most accurate results is any method of numerical integration of such integrals [4, 5, 21, 24, 33, 37]. A variety of methods have been proposed that could be roughly divided into a group of methods of direct integration (integration along the real axis), and a group of methods that consider changing of the integration path in the complex plane. The second approach considers approximate solving of these integrals using different methods, [6, 9, 11–15, 18, 19, 22, 25–32, 35, 36]. The reflection coefficient method, the method of images, methods considering approximation of the transformed reflection coefficient (spectral reflection coefficient - SRC) that is a part of the integrand, are some of the directions that researchers took in this area.

For the cases of wires buried in the ground, the influence of the air/ground boundary surface is usually taken into account using the reflection coefficient (or the transmission coefficient) approach (RC or TC, respectively, [5, 12–18, 20]), or the modified image theory (MIT, [15, 18, 19]). The latter one can only account for the electrical properties of the ground, not the burial depth, and its validity is frequency dependent (up to 1 MHz), [16]. On the other hand, the simplicity of the MIT and low computational cost that comes with it are also present in the RC or TC approaches; however, the plane wave incidence angle and wire depth are here taken into account. A drawback of these approaches is that they are valid for the far-field region, whereas the influence of the lossy ground is primarily noticeable in the close proximity of the sources. As an improvement, in [36] authors propose an approximation of the Sommerfeld integrals using a linear combination of 15 exponential functions with certain unknown constants obtained using the least-squares method. According to the authors, the maximum relative error of calculations is less than 0.1 per cent in a wide range of tested parameters describing the geometry and the ground, [36].

Similar solution, but applicable to static and quasi-static cases, is used in [11, 35]. The integrands are approximated by a set of exponential functions with unknown exponents and weight coefficients.

In this paper the authors propose a new model for approximation of one type of Sommerfeld integrals occurring in cases of conductors buried at arbitrary depth in the lossy ground parallel to the air/ground surface. This model is based on the procedure proposed by the first author in [25–32], which considers approximation of a part of the integrand using a weighted exponential function with an additional unknown complex constant term. This procedure has been successfully employed for approximation of two forms of Sommerfeld integrals appearing in expressions describing the Hertz's vector potential in the surroundings of sources positioned in the air above lossy ground. Proposed solutions have been applied to near- and far-field analysis of different wire antenna structures arbitrarily located in the air above lossy soil, [25–32], and modeling of the lightning discharge using an antenna model, [9].

Application of the newly proposed approximation of the integral in question is validated analyzing a centrally fed horizontal conductor immersed in the lossy ground. An integral equation of Hallén's type (HIE) is solved applying the point-matching method (PMM) as in [25–32], and adopting the polynomial current approximation as in [21, 22, 25–32]. Different burial depths of the wire, and different ground types, are considered at various frequencies. Obtained results are, were possible, compared to the TC approach in combination with the PMM solution to the HIE. Also, Partial Element Equivalent Circuit (PEEC) method applied in [10], and a so-called Hybrid Circuit Model (HCM) proposed in [7, 8], are also used for comparison purposes. Based on presented results, corresponding conclusions are given, and possibilities for further research are discussed.

3.2 Problem Formulation

Let us observe a centrally fed horizontal thin-wire conductor with lengths of conductor halves l, and cross-section radii a, buried in the lossy half-space (LHS) at depth h, as illustrated in Fig. 3.1. The LHS is considered a homogeneous, linear and isotropic medium of known electrical parameters. Electrical parameters of the air are:

- $\sigma_0 = 0$ - conductivity;
- ε_0 - permittivity;
- μ_0 - permeability,

and of the soil:

- σ_1 - conductivity;
- $\varepsilon_1 = \varepsilon_{r1}\varepsilon_0$ - permittivity (ε_{r1} - relative permittivity);
- $\mu_1 = \mu_0$ - permeability;
- $\underline{\sigma}_i = \sigma_i + j\omega\varepsilon_1$ - complex conductivity;

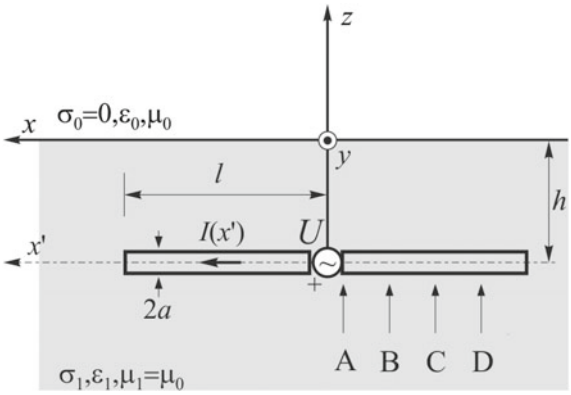

Fig. 3.1 Illustration of a horizontal conductor buried in the lossy half-space

- $\gamma_i = \alpha_i + \mathrm{j}\beta_i = (\mathrm{j}\omega\mu\underline{\sigma}_i)^{1/2},\ i = 0,\ 1$ - complex propagation constant ($i = 0$ for the air, and $i = 0$ for the LHS);
- $\omega = 2\pi f$ - angular frequency;
- $\underline{\varepsilon}_{r1}$ - complex relative permittivity;
- $\underline{n} = \gamma_1/\gamma_0 = \varepsilon_{r1}^{1/2} = (\varepsilon_{r1} - j60\sigma_1\lambda_0)^{1/2}$ - refractive index, and
- λ_0 - wavelength in the air.

The Hertz's vector potential has two components at an arbitrary point $M_1(x, y, z)$ in the ground in the vicinity of the conductor, i.e. $\mathbf{\Pi}_1 = \Pi_{x1}\hat{x} + \Pi_{z1}\hat{z}$, [5, 12–16, 18–20, 34]. Consequently, the tangential component of the scattered electric field can be expressed as:

$$E_{x1}^{sct}(x, x') = \left[\frac{\partial^2}{\partial x^2} - \underline{\gamma}_1^2\right]\Pi_{x1} + \frac{\partial^2\Pi_{z1}}{\partial x \partial z}, \tag{3.1}$$

where

$$\Pi_{x1} = \frac{1}{4\pi\underline{\sigma}_1}\int_{-l}^{l} I(x')\left[K_o(x, x') - K_i(x, x') + U_{11}\right]\mathrm{d}x', \tag{3.2}$$

$$\Pi_{z1} = \frac{1}{4\pi\underline{\sigma}_1}\int_{-l}^{l} I(x')\frac{\partial W_{11}}{\partial x}\mathrm{d}x', \tag{3.3}$$

with $I(x')$ - the current distribution along the conductor (x'- axis assigned to the wire);

$$K_o(x, x') = e^{-\underline{\gamma}_1 r_o},\ r_o = \sqrt{\rho^2 + a^2},\ \rho = \left|x - x'\right|, \tag{3.4}$$

$$K_i(x, x') = e^{-\underline{\gamma}_1 r_i},\ r_i = \sqrt{\rho^2 + (2h)^2},\ \rho = \left|x - x'\right|, \tag{3.5}$$

$$U_{11} = \int_{\alpha=0}^{\infty}\tilde{T}_{\eta 1}(\alpha)e^{-u_1(z+h)}\frac{\alpha}{u_1}J_0(\alpha\rho)\mathrm{d}\alpha, \tag{3.6}$$

$$W_{11} = \int_{\alpha=0}^{\infty} \tilde{T}_{\eta 2}(\alpha) e^{-u_1(z+h)} \frac{\alpha}{u_1} J_0(\alpha\rho) \mathrm{d}\alpha, \tag{3.7}$$

$$\tilde{T}_{\eta 1}(\alpha) = \frac{2u_1}{u_0 + u_1}, \; u_i = \sqrt{\alpha^2 + \underline{\gamma}_i^2}, \; i = 0, 1, \tag{3.8}$$

$$\tilde{T}_{\eta 2}(\alpha) = \frac{2u_1(u_0 - u_1)}{\underline{\gamma}_1^2 u_0 + \underline{\gamma}_0^2 u_1}, \; u_i = \sqrt{\alpha^2 + \underline{\gamma}_i^2}, \; i = 0, 1, \tag{3.9}$$

where $J_0(\alpha\rho)$ is the zero-order Bessel function of the first kind. Adopting (3.2) and (3.3), expression (3.1) can be written as

$$E_{x1}^{sct}(x, x') = \frac{1}{4\pi \underline{\sigma}_1} \int_{-l}^{l} I(x') G(x, x') \mathrm{d}x', \text{ and} \tag{3.10}$$

$$G(x, x') = \left[\frac{\partial^2}{\partial x^2} - \underline{\gamma}_1^2 \right] \left[K_o(x, x') - K_i(x, x') + U_{11} \right] + \frac{\partial^2}{\partial x \partial z} \left[\frac{\partial W_{11}}{\partial x} \right]. \tag{3.11}$$

Since, according to [34], integral given by (3.7) can be rewritten as $\frac{\partial W_{11}}{\partial z} = -\underline{\gamma}_1^2 V_{11} - U_{11}$, where

$$V_{11} = \int_{\alpha=0}^{\infty} \tilde{T}_{\eta 3}(\alpha) e^{-u_1(z+h)} \frac{\alpha}{u_1} J_0(\alpha\rho) \mathrm{d}\alpha, \text{ and} \tag{3.12}$$

$$\tilde{T}_{\eta 3}(\alpha) = \frac{2u_1}{\underline{\gamma}_1^2 u_0 + \underline{\gamma}_0^2 u_1}, \; u_i = \sqrt{\alpha^2 + \underline{\gamma}_i^2}, \; i = 0, 1, \tag{3.13}$$

then the expressions (3.10) and (3.11) can be rewritten as

$$E_{x1}^{sct}(x, x') = \frac{1}{4\pi \underline{\sigma}_1} \begin{bmatrix} \frac{\partial^2}{\partial x^2} \int_{-l}^{l} I(x') \left[K_o(x, x') - K_i(x, x') - \underline{\gamma}_1^2 V_{11} \right] \mathrm{d}x' - \\ -\underline{\gamma}_1^2 \int_{-l}^{l} I(x') \left[K_o(x, x') - K_i(x, x') + U_{11} \right] \mathrm{d}x' \end{bmatrix}. \tag{3.14}$$

Boundary condition for the total tangential component of the electric field vector must be satisfied at any given point on the conductor's surface, and if the wire is perfectly conducting then

$$E_{x1}^{sct}(x, x') + E_{x1}^{tr}(x, x') = 0, \tag{3.15}$$

where $E_{x1}^{tr}(x, x')$ is the transmitted electric field. Now, the integral equation-IE (3.15) has the form

$$E_{x1}^{tr}(x, x') = -E_{x1}^{sct}(x, x'), \tag{3.16}$$

which, as a solution, gives the current distribution along the observed conductor. However, in order to do so, a group of improper integrals, referred to as integrals of Sommerfeld type, needs to be solved. Those would be integrals given by (3.6) and (3.7) if the formulation (3.10) and (3.11) is substituted in (3.16), or a set of integrals (3.6) and (3.12), if (3.14) is adopted.

3.3 Sommerfeld Integral Approximations

Different approaches have been applied in this field, but most of them start with a simplified version of the Green's function (3.11) having the following form:

$$G(x, x') = \left[\frac{\partial^2}{\partial x^2} - \underline{\gamma}_1^2\right]\left[K_o(x, x') - K_i(x, x') + U_{11}\right], \tag{3.17}$$

which means that only one Sommerfeld integral (the one given by (3.6)) needs to be solved. The following sub-sections will give an overview of a solution already proposed in the literature (Sect. 3.3.1), and also a newly developed one by the authors of this paper (Sect. 3.3.2).

3.3.1 Transmission Coefficient (TC) Approach

Transmission coefficient approach [3, 12], substitutes the part $-K_i(x,\ x') + U_{11}$ in (3.17) by

$$-K_i(x,\ x') + U_{11} = -K_i(x,\ x')\Gamma_{TM}^{trans.}, \tag{3.18}$$

i.e. approximates the U_{11} by

$$U_{11}^a \approx K_i(x,\ x')\left(1 - \Gamma_{TM}^{trans.}\right), \tag{3.19}$$

where

$$\Gamma_{TM}^{trans.} = \frac{2\underline{n}\cos\theta}{\underline{n}^2\cos\theta + \sqrt{\underline{n}^2 - \sin^2\theta}}, \theta = \arctan\frac{\rho}{2h}, \tag{3.20}$$

presents the transmission coefficient for TM polarization.

3.3.2 Two-Image Approximation - TIA

In this paper, the authors propose a new approximation for the integral (3.6), so-called two-image approximation (TIA) developed using the procedure applied in [25–32] for modeling two different forms of Sommerfeld integrals occurring in cases of sources located in the air above LHS.

1st case: Let us assume the expression (3.8) in the following form:

$$\tilde{T}^a_{\eta 1} = \underline{B} + \underline{A} e^{-(u_1 - \underline{\gamma}_1)\underline{d}}, \tag{3.21}$$

where $\underline{B}$, $\underline{A}$ and $\underline{d}$ are unknown complex constants. When (3.21) is substituted into (3.6), taking into account the identity, [23],

$$\int_{\alpha=0}^{\infty} \frac{e^{-|c|\sqrt{\alpha^2+\underline{\gamma}_1^2}}}{\sqrt{\alpha^2+\underline{\gamma}_1^2}} \alpha \, J_0(\alpha\rho) \mathrm{d}\alpha = K_c(x,x') = \frac{e^{-\underline{\gamma}_1\sqrt{\rho^2+|c|^2}}}{\sqrt{\rho^2+|c|^2}}, \tag{3.22}$$

the following general TIA approximation of (3.6) is obtained:

$$U^a_{11}(x,x') = \underline{B} K_{zh}(x,x') + \underline{A} e^{\underline{\gamma}_1 |\underline{d}|} K_{zhd}(x,x'), \tag{3.23}$$

where

$$K_{zh}(x,x') = e^{-\underline{\gamma}_1 r_{zh}}, \; r_{zh} = \sqrt{\rho^2 + (z+h)^2}, \tag{3.24}$$

$$K_{zhd}(x,x') = e^{-\underline{\gamma}_1 r_{zhd}}, \; r_{zhd} = \sqrt{\rho^2 + (z+h+|\underline{d}|)^2}. \tag{3.25}$$

Constants $\underline{B}$, $\underline{A}$ and $\underline{d}$ are evaluated matching the expressions (3.8) and (3.21), as well as their first derivative, at certain characteristic points in the range of integration of (3.6). One possibility is as follows,

1. Matching point 1: $u_1 \to \infty$

$$\tilde{T}_{\eta 1}(u_1 \to \infty) = 1, \tag{3.26}$$

$$\tilde{T}^a_{\eta 1}(u_1 \to \infty) = \underline{B}. \tag{3.27}$$

2. Matching point 2: $u_1 = \underline{\gamma}_0$

$$\tilde{T}_{\eta 1}(u_1 = \underline{\gamma}_0) = \frac{2}{1+\sqrt{2-\underline{n}^2}}, \tag{3.28}$$

$$\tilde{T}^a_{\eta 1}(u_1 = \underline{\gamma}_0) = \underline{B} + \underline{A} e^{-\underline{\gamma}_0(1-\underline{n})\underline{d}}. \tag{3.29}$$

3. Matching point for the first derivative: $u_1 = \underline{\gamma}_0$

$$\tilde{T}'_{\eta 1}(u_1 = \underline{\gamma}_0) = \frac{-2(\underline{n}^2 - 1)}{\underline{\gamma}_0 \sqrt{2 - \underline{n}^2} \left(1 + \sqrt{2 - \underline{n}^2}\right)^2}, \tag{3.30}$$

$$\tilde{T}'^{a}_{\eta 1}(u_1 = \underline{\gamma}_0) = -\underline{d}\,\underline{A} e^{-\underline{\gamma}_0 (1 - \underline{n}) \underline{d}}. \tag{3.31}$$

Equating (3.26) and (3.27), (3.28) and (3.29), and (3.30) and (3.39), a system of three equations over three unknown constants $\underline{B}$, $\underline{A}$ and $\underline{d}$ is formed, and the solution is given in the first row of Table 3.1.

2nd case: The same approximation of (3.6) can be achieved if we assume (3.8) as

$$\tilde{T}^a_{\eta 1} = \underline{B} + \underline{A} e^{-u_1 \underline{d}}, \tag{3.32}$$

then (3.6) gets the form

$$U^a_{11}(x, x') = \underline{B} K_{zh}(x, x') + \underline{A} K_{zhd}(x, x'), \tag{3.33}$$

For the same matching points as previously, we get
1. Matching point 1: $u_1 \to \infty$

$$\tilde{T}_{\eta 1}(u_1 \to \infty) = 1, \tag{3.34}$$

$$\tilde{T}^a_{\eta 1}(u_1 \to \infty) = \underline{B}. \tag{3.35}$$

2. Matching point 2: $u_1 = \underline{\gamma}_0$

$$\tilde{T}_{\eta 1}(u_1 = \underline{\gamma}_0) = \frac{2}{1 + \sqrt{2 - \underline{n}^2}}, \tag{3.36}$$

$$\tilde{T}^a_{\eta 1}(u_1 = \underline{\gamma}_0) = \underline{B} + \underline{A} e^{-\underline{\gamma}_0 \underline{d}}. \tag{3.37}$$

3. Matching point for the first derivative: $u_1 = \underline{\gamma}_0$

$$\tilde{T}'_{\eta 1}(u_1 = \underline{\gamma}_0) = \frac{-2(\underline{n}^2 - 1)}{\underline{\gamma}_0 \sqrt{2 - \underline{n}^2} \left(1 + \sqrt{2 - \underline{n}^2}\right)^2}, \tag{3.38}$$

$$\tilde{T}'^{a}_{\eta 1}(u_1 = \underline{\gamma}_0) = -\underline{d}\,\underline{A} e^{-\underline{\gamma}_0 \underline{d}}. \tag{3.39}$$

The values obtained for $\underline{B}$, $\underline{A}$ and $\underline{d}$ are listed in the second row of Table 3.1.

Table 3.1 Obtained values of constants describing proposed TIA model

TIA Model	$\underline{B}$	$\underline{A}$	$\underline{d}$
$1^{st}case$	1	$\frac{1-\sqrt{2-\underline{n}^2}}{1+\sqrt{2-\underline{n}^2}} e^{\underline{\gamma}_0(1-\underline{n})\underline{d}}$	$\frac{2}{\underline{\gamma}_0\sqrt{2-\underline{n}^2}}$
$2^{nd}case$	1	$\frac{1-\sqrt{2-\underline{n}^2}}{1+\sqrt{2-\underline{n}^2}} e^{\underline{\gamma}_0\underline{d}}$	$\frac{2}{\underline{\gamma}_0\sqrt{2-\underline{n}^2}}$

3.4 Solution of the Integral Equation

In order to validate the application of the proposed approximation for the integral (3.6), the integral equation (3.16) will be solved for the current. First, the form of the Hallén's IE (HIE) is obtained as a solution of the partial differential equation that arises from (3.16). For the case of a thin-wire conductor centrally-fed by a Dirac's δ-generator, $E^{tr}_{x1}(x, x') = U\delta(x)$, $U = 1$ V, and taking into account the simplified Green's function given by (3.17), the HIE becomes:

$$\int_{-l}^{l} I(x')\left[K_o(x, x') - K_i(x, x') + U_{11}\right] \mathrm{d}x' - C\cos(\mathrm{j}\underline{\gamma}_1 x) = \mathrm{j}\frac{\underline{n}}{60} U \sin(\mathrm{j}\underline{\gamma}_1 x), \tag{3.40}$$

where C is an integration constant.

In order to solve (3.40), the point-matching method (PMM) is applied, giving us a system of linear equations with current distribution and integration constant C as unknowns. In this paper, we adopt the entire domain polynomial current approximation for the current as in [21, 22, 25–32]:

$$I(u' = x'/l) = \sum_{m=0}^{M} I_m u'^m, \ 0 \le u' \le 1, \tag{3.41}$$

where $I_m, m = 0,\ 1, ...,\ M$, are complex current coefficients. This amounts to a total of $(M + 1) + 1$ unknowns, which calls for as much linear equations. The matching is done at $(M + 1)$ points that are chosen as $x_i = il/M$, $i = 0,\ 1,\ 2, ...,\ M$. This way, a system of $(M + 1)$ linear equations is formed, lacking one additional equation to account for the unknown integration constant C. This remaining linear equation is obtained applying the condition for vanishing of the current at the conductor's end, which corresponds to $I(-l) = I(l) = 0$. If we adopt TC or TIA model for (3.6), the system of equations becomes:

$$\sum_{m=0}^{M} I_m \int_{-l}^{l} \left(\frac{x'}{l}\right)^m \left[K_o(x, x') - K_i(x, x') + U^a_{11}(x, x')\right] \mathrm{d}x' - C\cos(\beta_0 \underline{n} x_i) = \\ = -\mathrm{j}\frac{\underline{n}}{60} U \sin(\beta_0 \underline{n} x_i),\ i = 0,\ 1,\ 2, ...,\ M, \tag{3.42}$$

$$\sum_{m=0}^{M} I_m = 0. \tag{3.43}$$

3.5 Numerical Results

First we observed the convergence of the PMM method when the TIA approach to solving Sommerfeld integral (3.6) is adopted. The current magnitude is calculated for different values of the order of the polynomial current distribution M. Obtained results along a half of the conductor, which correspond to burial depth of $h = 0.1$ m, can be observed from Figs. 3.2 and 3.3 for two frequency values: 1 and 10 MHz, respectively. Each figure includes two diagrams corresponding to two different values of the ground conductivity: (a) $\sigma_1 = 0.001$ S/m and (b) $\sigma_1 = 0.01$ S/m. The analysis is performed for the case of the conductor's half-length $l = 5$ m, cross-section radius $a = 5$ mm, and electric permittivity of the ground $\varepsilon_{r1} = 10$.

The conductor with the same geometry parameters is considered again, for two cases of burial depths: (a) $h = 1.0$ m and (b) $h = 5.0$ m. The variable parameter in all figures is the specific conductivity of the ground, and it takes three values: $\sigma_1 = 0.001, 0.01$ and 0.1 S/m. The analysis is performed for the case of the electric permittivity of the ground $\varepsilon_{r1} = 10$. The results obtained by the PMM method and both the TC and newly proposed TIA approach are compared to the corresponding ones obtained by the methods from [7, 8, 10]. In [10] the authors employ the Partial Element Equivalent Circuit (PEEC) method, while in [7, 8] a so-called Hybrid Circuit Model (HCM) is proposed. Satisfying accordance of the results can be observed from the presented results. This is especially noticeable for more deeply buried conductors, and lower frequencies.

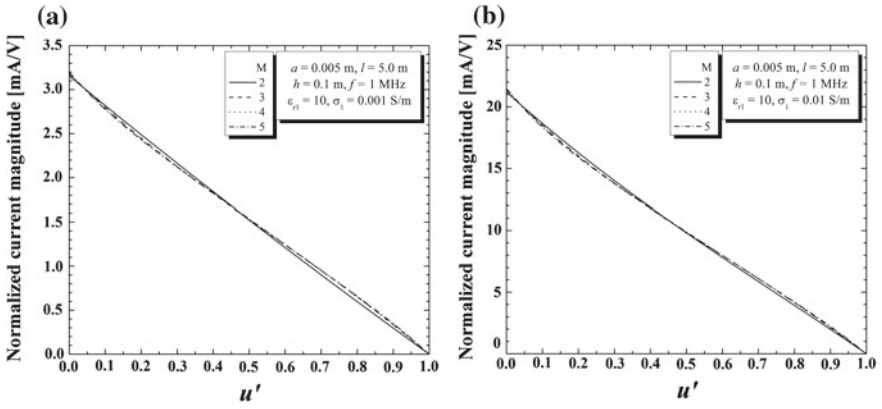

Fig. 3.2 Current magnitude along a half of the conductor for burial depth of 0.1 m and two values of ground conductivities: **a** 0.001 S/m, **b** 0.01 S/m. Order of polynomial current approximation M is taken as a parameter. Frequency is 1 MHz

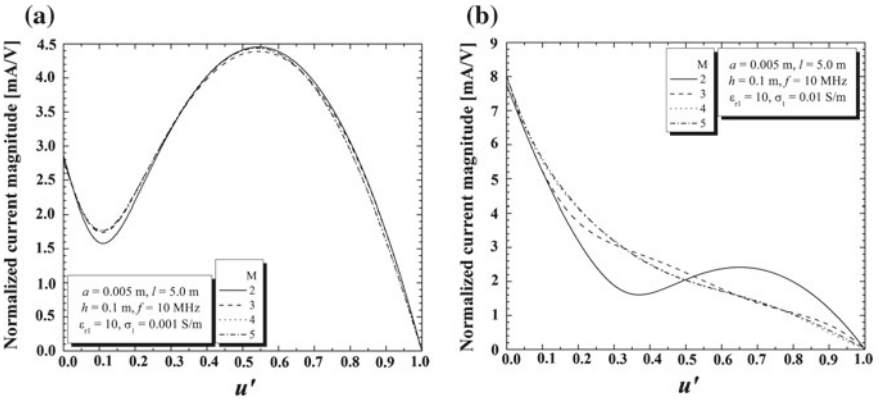

Fig. 3.3 Current magnitude along a half of the conductor for burial depth of 0.1 m and two values of ground conductivities: **a** 0.001 S/m, **b** 0.01 S/m. Order of polynomial current approximation M is taken as a parameter. Frequency is 10 MHz

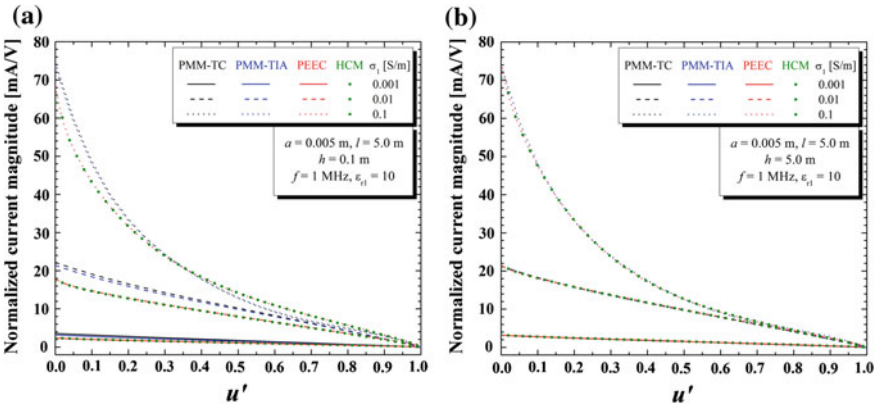

Fig. 3.4 Current magnitude along a half of the conductor buried at **a** 0.1 m, **b** 5 m for frequency of 1 MHz. Conductivity of the ground is taken as a parameter. Comparison of different methods

Next, results for the current magnitude are given in Figs. 3.4 and 3.5 for two frequency values, 1 and 10 MHz, respectively.

Figures 3.6, 3.7 and 3.8 illustrate the current magnitude distribution for three different frequencies: 1, 5 and 10 MHz. Two cases of burial depth are considered: (a) $h = 1.0$ m and (b) $h = 5.0$ m. The conductor's geometrical parameters are the same as previously.

Each figure corresponds to the same electrical permittivity ($\varepsilon_{r1} = 10$), while the ground's conductivity is varied ($\sigma_1 = 0.001, 0.01$ and 0.1 S/m). Again, the results obtained by different methods, PMM-TC, PMM-TIA, PEEC, and HCM, are compared.

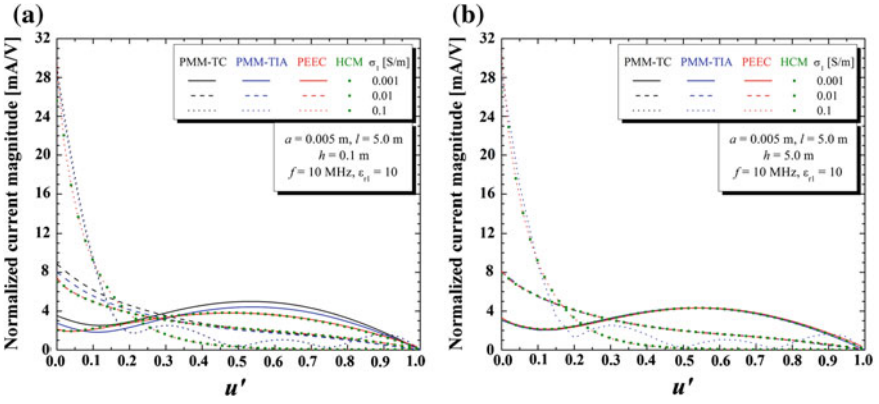

Fig. 3.5 Current magnitude along a half of the conductor buried at **a** 0.1 m, **b** 5 m for frequency of 10 MHz. Conductivity of the ground is taken as a parameter. Comparison of different methods

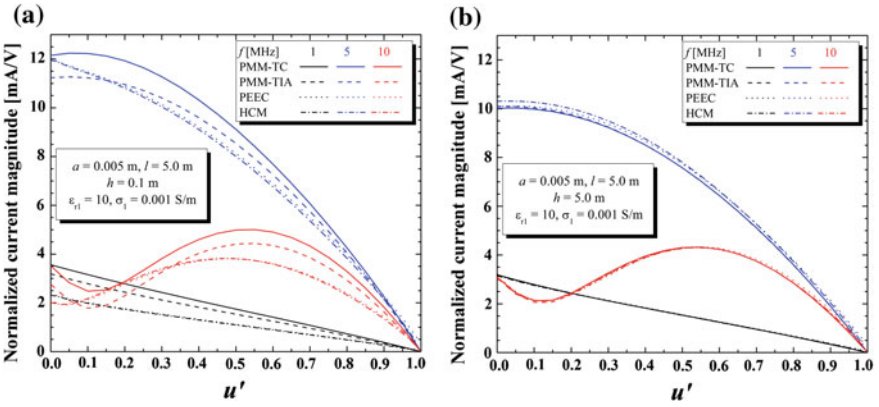

Fig. 3.6 Current magnitude along a half of the conductor buried at **a** 0.1 m and **b** 5 m for ground conductivity of 0.001 S/m. Frequency is taken as a parameter. Comparison of different methods

Final set of numerical results illustrates the influence of different values of the electrical permittivity at two frequencies: (a) 1 MHz and (b) 5 MHz. Figures 3.9, 3.10 and 3.11 correspond to three cases of specific ground conductivity $\sigma_1 = 0.001$ S/m, 0.01 S/m, and 0.1 S/m. The conductor has the same geometry as previously, and is positioned at $h = 5.0$ m below the boundary surface air/LHS. The results obtained by the PMM-TIA (solid squares), and the PEEC method (continual lines) are presented. Observed values of the electrical permittivity are: $\varepsilon_{r1} = 1, 2, 5, 10, 20, 36$ and 81. This influence is most noticeable at higher frequencies and for lower values of the ground conductivity.

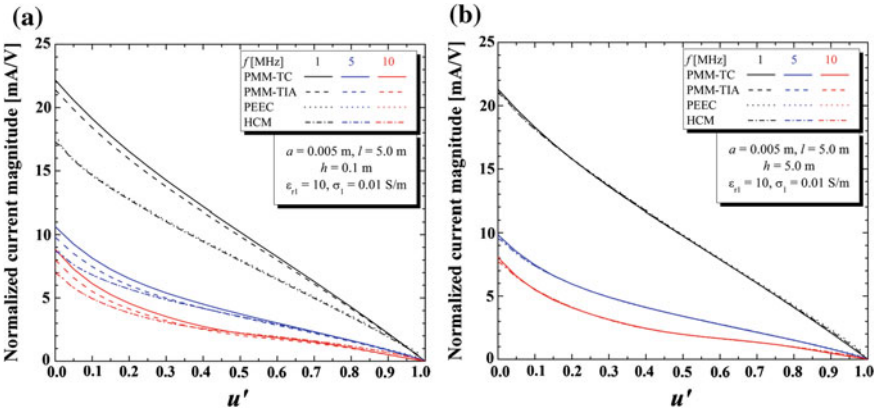

Fig. 3.7 Current magnitude along a half of the conductor buried at **a** 0.1 m and **b** 5 m for ground conductivity of 0.01 S/m. Frequency is taken as a parameter. Comparison of different methods

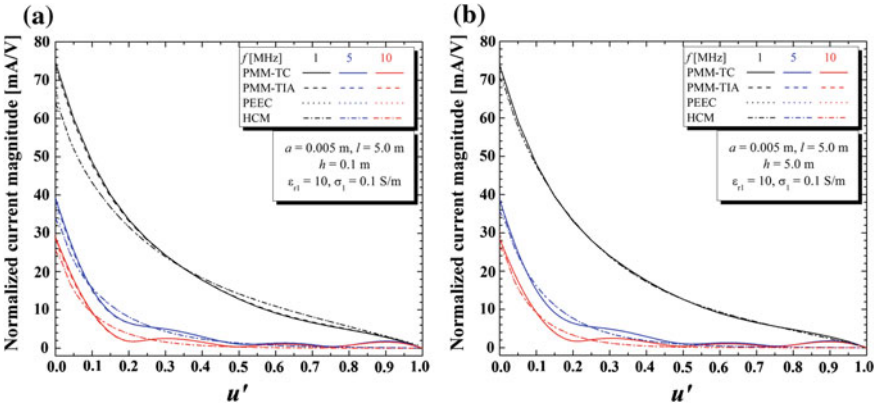

Fig. 3.8 Current magnitude along a half of the conductor buried at **a** 0.1 m and **b** 5 m for ground conductivity of 0.1 S/m. Frequency is taken as a parameter. Comparison of different methods

3.6 Conclusion

The aim of the paper to effectively approximate one form of Sommerfeld integrals has been achieved developing a simple approximation in a form of a weighted exponential function with an additional constant term, denoted here as two-image approximation (TIA). Proposed approximation is valid over a wide range of parameters (electrical parameters of the ground and geometry parameters). Presented numerical results show that the proposed model in combination with the PMM method can be successfully applied to frequency analysis of conductors buried in the lossy medium.

Furthermore, presented results indicate a possibility of effective application of the proposed procedure to other forms of Sommerfeld integrals that also appear

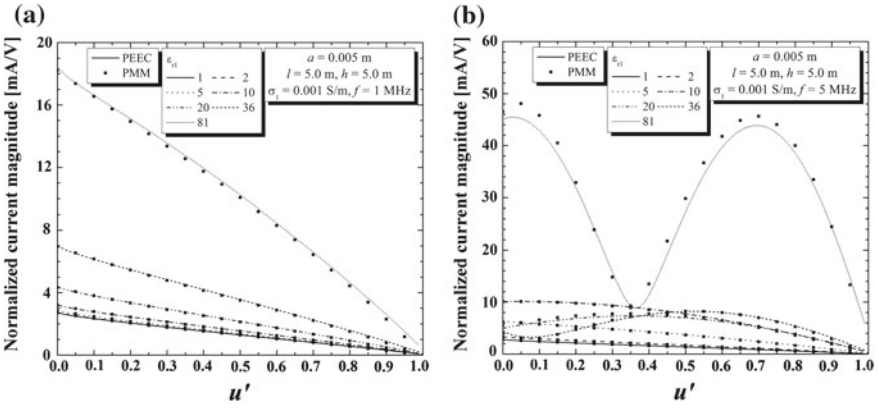

Fig. 3.9 Current magnitude along a half of the conductor for frequencies **a** 1 MHz, **b** 5 MHz. Electrical permittivity of the ground is taken as a parameter. Ground conductivity is 0.001 S/m

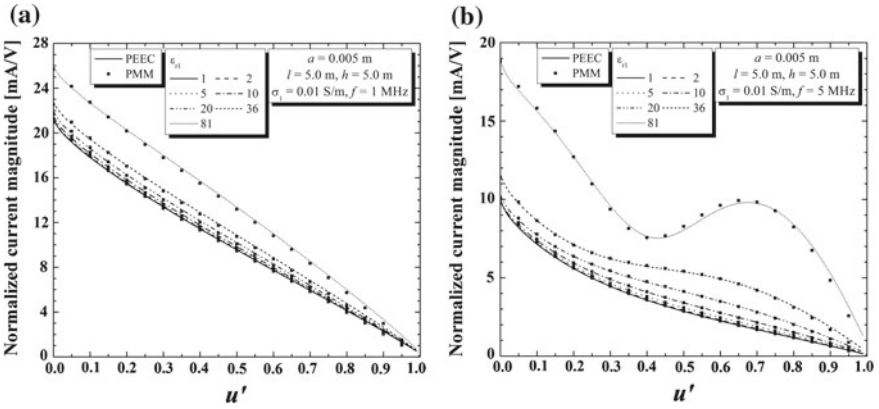

Fig. 3.10 Current magnitude along a half of the conductor for frequencies **a** 1 MHz, **b** 5 MHz. Electrical permittivity of the ground is taken as a parameter. Ground conductivity is 0.01 S/m

in the observed case of sources buried in the lossy ground (the ones given by (3.7) and (3.12)), which are usually neglected [3, 5, 6, 12–20, 24]. This would yield a more stringent analysis, and also a more accurate one, of not only antennas immersed in the lossy ground, but also wire grounding systems in such soil, buried telecommunication cables exposed to electromagnetic interferences, submarine dipoles, bare or isolated antennas embedded in dissipative media, etc.

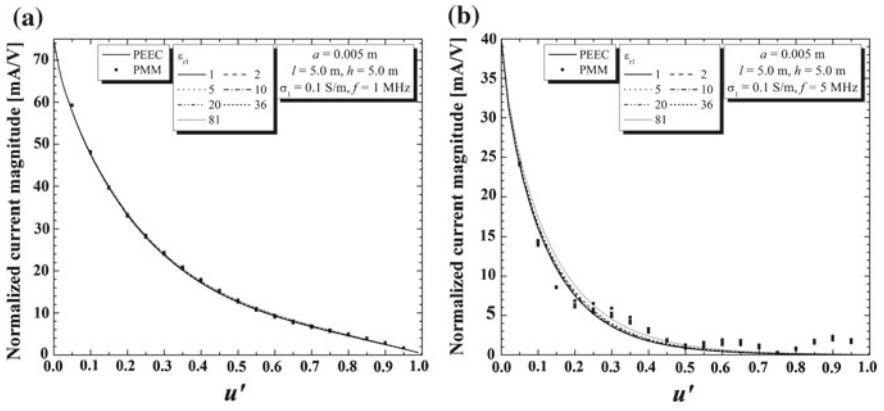

Fig. 3.11 Current magnitude along a half of the conductor for frequencies **a** 1 MHz, **b** 5 MHz. Electrical permittivity of the ground is taken as a parameter. Ground conductivity is 0.1 S/m

References

1. Arnautovski-Toseva, V., Drissi, K.E.K., Kerroum, K.: HF comparison of image and TL models of a horizontal thin-wire conductor in finitely conductive earth. In: Proceedings of SOFTCOM 2011, Split, Croatia, pp. 1–5 (2011)
2. Banos, A.: Dipole Radiation in the Presence of a Conducting Half-Space. Pergamon Press, New York (1966)
3. Bridges, G.E.: Transient plane wave coupling to bare and insulated cables buried in a lossy half-space. IEEE Trans. EMC **37**(1), 62–70 (1995)
4. Burke, G.J., Miller, E.K.: Modeling antennas near to and penetrating a lossy interface. IEEE Trans. AP **32**(10), 1040–1049 (1984)
5. Grcev, L., Dawalibi, F.: An electromagnetic model for transients in grounding systems. IEEE Trans. Power Deliv. **5**(4), 1773–1781 (1990)
6. Grcev, L.D., Menter, F.E.: Transient electro-magnetic fields near large earthing systems. IEEE Trans. Magn. **32**(3), 1525–1528 (1996)
7. Jankoski, R., Kuhar, A., Grcev, L.: Frequency domain analysis of large grounding systems using hybrid circuit model. In: Proceedings of 8th International Ph.D. Seminar on Computational and Electromagnetic Compatibility - CEMEC 2014, Timisora, Romania, pp. 1–4 (2014)
8. Jankoski, R., Kuhar, A., Markovski, B., Kacarska, M., Grcev, L.: Application of the electric circuit approach in the analysis of grounding conductors. In: Proceedings of 5th International Symposium on Applied Electromagnetics - SAEM 2014, Skopje, Macedonia, pp. 1–7 (2014)
9. Javor, V., Rančić, P.D.: Electromagnetic field in the vicinity of lightning protection rods at a lossyground. IEEE Trans. EMC **51**(2), 320–330 (2009)
10. Kuhar, A., Jankoski, R., Arnautovski-Toseva, V., Ololoska-Gagoska, L., Grcev, L.: Partial element equivalent circuit model for a perfect conductor excited by a current source. CD Proceedings of 11th International Conference on Applied Electromagnetics - PES 2013,Niš, Serbia, pp. 1–4 (2013)
11. Poljak, D.: New numerical approach in the analysis of a thin wire radiating over a lossy half-space. Int. J. Numer. Methods Eng. **38**(22), 3803–3816 (1995)
12. Poljak, D.: Electromagnetic modeling of finite length wires buried in a lossy half-space. Eng. Anal. Bound. Elem. **26**(1), 81–86 (2002)
13. Poljak, D., Doric, V.: Time domain modeling of electromagetic filed coupling to finite length wires embedded in a dielectric half-space. IEEE Trans. EMC **47**(2), 247–253 (2005)

14. Poljak, D., Doric, V.: Wire antenna model for transient analysis of simple grounding systems, Part II: The horizontal grounding electrode. Progress Electromagn. Res. **64**, 167–189 (2006)
15. Poljak, D., Gizdic, I., Roje, V.: Plane wave coupling to finite length cables buried in a lossy ground. Eng. Anal. Bound. Elem. **26**(9), 803–806 (2002)
16. Poljak, D., Doric, V., Drissi, K.E.K., Kerroum, K., Medic, I.: Comparison of wire antenna and modified transmission line approach to the assessment of frequency response of horizontal grounding electrodes. Eng. Anal. Bound. Elem. **32**(8), 676–681 (2008)
17. Poljak, D., Doric, V., Rachidi, F., Drissi, K.E.K., Kerroum, K., Tkatchenko, S., et al.: Generalized form of telegrapher's equations for the electromagnetic field coupling to buried wires of finite length. IEEE Trans. EMC. **51**(2), 331–337 (2009)
18. Poljak, D., Sesnic, S., Goic, R.: Analytical versus boundary element modelling of horizontal ground electrode. Eng. Anal. Bound. Elem. **34**(4), 307–314 (2010)
19. Poljak, D., Drissi, K.E.K., Kerroum, K., Sesnic, S.: Comparison of analytical and boundary element modeling of electromagnetic field coupling to overhead and buried wires. Eng. Anal. Bound. Elem. **35**(3), 555–563 (2011)
20. Poljak, D., Lucic, R., Doric, V., Antonijevic, S.: Frequency domain boundary element versus time domain finite element model for the transient analysis of horizontal grounding electrode. Eng. Anal. Bound. Elem. **35**(3), 375–382 (2011)
21. Popović, B.D., Djurdjević, D.: Entire-domain analysis of thin-wire antennas near or in lossy ground. IEE Proc. Microw. Antennas Propag. **142**(3), 213–219 (1995)
22. Popović, B.D., Petrović, V.V.: Horizontal wire antenna above lossy half-space: simple accurate image solution. Int. J. Numer. Model.: Electron. Netw. Devices Fields **9**(3), 194–199 (1996)
23. Prudnikov, A.P., Brychkov, YuA, Marichev, O.I.: Integrals and Series: Special Functions, vol. 2, p. 189. CRC Press, Florida (1998)
24. Rahmat-Samii, Y., Parhami, P., Mittra, R.: Loaded horizontal antenna over an imperfect ground. IEEE Trans. AP **26**(6), 789–796 (1978)
25. Rančić, M. P., Aleksić, S.: Simple numerical approach in analysis of horizontal dipole antennas above lossy half-space. IJES - Int. J. Emerg. Sci. 1(4), 586–596 [PES 2011, Serbia, 2011, paper no. O4–3] (2011)
26. Rančić, M.P., Aleksić, S.: Simple approximation for accurate analysis of horizontal dipole antenna above a lossy half-space. Proceedings of 10th International Conference on Telecommunications in Modern Satellite. Cable and Broadcasting Services - TELSIKS 2011, pp. 432–435. Niš, Serbia (2011)
27. Rančić, M. P., Aleksić, S.: Horizontal dipole antenna very close to lossy half-space surface. Electrical Review. **7b**, 82–85 (2012) [ISEF 2011, Portugal, 2011, PS.4.19]
28. Rančić, M. P., Aleksić, S.: Analysis of wire antenna structures above lossy homogeneous soil. In: Proc. of 21st Telecommunications Forum (TELFOR), pp. 640–647, Belgrade, Serbia, (2013)
29. Rančić, M.P., Rančić, P.D.: Vertical linear antennas in the presence of a lossy half-space: An improved approximate model. Int. J. Electron. Commun. AEUE **60**(5), 376–386 (2006)
30. Rančić, M.P., Rančić, P.D.: Vertical dipole antenna above a lossy half-space: efficient and accurate two-image approximation for the Sommerfeld integral. In: CD Proceedings of EuCAP'06, paper No121, Nice, France (2006)
31. Rančić, M.P., Rančić, P.D.: Horizontal linear antennas above a lossy half-space: a new model for the Sommerfeld's integral kernel. Int. J. Electron. Commun. AEUE **65**(10), 879–887 (2011)
32. Rančić, M.P., Aleksić, S., Khavanova, M.A., Petrov, R.V., Tatarenko, A.S., Bichurin, M.I.: Analysis of symmetrical dipole antenna on the boundary between air and lossy half-space. Mod. Probl. Sci. Educ. **6**, 1–7 (2012). (in Russian)
33. Sarkar, T.K.: Analysis of arbitrarily oriented thin wire antennas over a plane imperfect ground. Int. J. Electron. Commun. (AEUE) **31**, 449–457 (1977)
34. Siegel, M., King, R.W.P.: Radiation from linear antennas in a dissipative half-space. IEEE Trans. AP **19**(4), 477–485 (1971)
35. Vujević, S., Kurtović, M.: Efficient use of exponential approximation of the kernel function in interpretation of resistivity sounding data. Int. J. Eng. Model. **5**(1–2), 45–52 (1992)

36. Vujević, S., Sarajcev, I.: A new algorithm for exponential approximation of Sommerfeld integrals. In: Proceedings of 11th Int. DAAM Symp. on Intelligent Manufacturing and Automation: Man - Machine - Nature, pp. 485–486, Vienna, Austria, (2000)
37. Zou, J., Zhang, B., Du, X., Lee, J., Ju, M.: High-efficient evaluation of the lightning electromagnetic radiation over a horizontally multilayered conducting ground with a new complex integration path. IEEE Trans. on EMC. **PP(99)**, 1–9 (2014)